Journal of Materials Chemistry B

ROYAL SOCIETY OF CHEMISTRY

PAPER

View Article Online
View Journal | View Issue

Cite this: J. Mater. Chem. B, 2021, 9, 3200

A colon-targeted podophyllotoxin nanoprodrug: synthesis, characterization, and supramolecular hydrogel formation for the drug combination†

Wei Ha,‡[a] Xiao-Bo Zhao,‡[a] Wei-Hua Zhao,[a] Jiang-Jiang Tang[b] and Yan-Ping Shi *[a]

Making full use of the undeveloped bioactive natural product derivatives by selectively delivering them to target sites can effectively increase their druggability and reduce the wastage of resources. Azo-based prodrugs are widely regarded as an effective targeted delivery means for colon-related disease treatment. Herein, we report a new-type of azo-based nanoprodrug obtained from bioactive natural products, in which the readily available podophyllotoxin natural products are connected with methoxy polyethylene glycol (mPEG) *via* a multifunctional azobenzene group. The amphiphilic prodrug can form nanosized micelles in water and will be highly selectively activated by azoreductases, leading to the *in situ* generation of anticancer podophyllotoxin derivatives (**AdP**) in the colon after the cleavage of the azo bond. To satisfy the demand of drug carriers for cancer combination therapy in clinics, α-CD is further introduced into this nanoprodrug micelle system to form a supramolecular hydrogel *via* a cascade self-assembly strategy. Using imaging mass spectrometry (IMS), the colon-specific drug release ability of the hydrogel after oral administration is demonstrated at the molecular level. Finally, the nanoprodrug hydrogel is further used as a carrier to load a hydrophilic anti-cancer drug 5-FU during the hierarchical self-assembly process and to co-deliver **AdP** and 5-FU for the drug combination. The combination use of **AdP** and 5-FU provides enhanced cytotoxicity which indicates a significant synergistic interaction. This work offers a new way to enhance the therapeutic effect of nanoprodrugs *via* drug combination, and provides a new strategy for reusing bioactive natural products and their derivatives.

Received 21st November 2020,
Accepted 9th March 2021

DOI: 10.1039/d0tb02719g

rsc.li/materials-b

Introduction

Compounds found in natural resources have abundant chemical structures and broad biological activities, and are the most important sources for drug discovery.[1–3] The structural modification and optimization of active natural products could greatly improve their druggability and pharmacological activity, which has been considered as a crucial strategy in natural product-based drug discovery.[4–7] In the past century, a large number of natural product derivatives have been synthesized for drug discovery. However, only a few of them have been successfully launched, while a huge number of other active derivatives were wasted due to their poor physicochemical properties. Taking podophyllotoxin as an example, at least 20 000 active derivatives have been reported, but only two of them are clinically applied.[8,9] Therefore, making full use of these undeveloped bioactive natural product derivatives can effectively increase their druggability and reduce the wastage of resources.

The prodrug strategy has received extensive attention in the structural modification of active natural products because of its significant advantages in improving the physicochemical properties.[10–12] One of the ultimate goals of the prodrug strategy is to deliver the drug to the target site with high specificity while minimizing the drug exposure of other organs by rational design.[13,14] Azo-based prodrugs provide an effective target delivery means for colon-related disease treatment.[15,16] The colonic microflora can specifically secrete azoreductase which has the ability to reduce the azobenzene group to the corresponding phenylamine.[17–19] Based on this unique character, many commonly used drugs, such as sulfasalazine, olsalazine and

[a] CAS Key Laboratory of Chemistry of Northwestern Plant Resources and Key Laboratory for Natural Medicine of Gansu Province, Lanzhou Institute of Chemical Physics, Chinese Academy of Sciences (CAS), Lanzhou 730000 People's Republic of China. E-mail: shiyp@licp.cas.cn

[b] Shaanxi Key Laboratory of Natural Products & Chemical Biology, College of Chemistry and Pharmacy, Northwest A&F University, Yangling, Shaanxi 712100 People's Republic of China

† Electronic supplementary information (ESI) available: General information, Tables S1 and S2, and supplementary Fig. S1–14. See DOI: 10.1039/d0tb02719g

‡ These authors contributed equally.

balsalazide, are used as a prodrug for the targeted release of active 5-ASA inside the colon.[20–22] The phenylamino group is present in various natural product derivatives, which include many highly active derivatives. However, most of them have not been further investigated since they were reported with some physicochemical defects arising from their molecular structure; this creates enormous wastage of compound resources.[23–26] We thus proposed that introducing an azobenzene group to these compounds *via* rational design of the molecular structure would provide the possibility to deliver them specifically to the colon for colon related disease treatment, resulting in more efficient utilization of the bioactive compounds which bear a phenylamino group. It is undeniable that azo-based prodrugs, especially amphiphilic nanoprodrugs, are attractive in anticancer compound delivery due to their potential in improving drug solubility, stability and accumulation at the target organ. However, although anticancer compounds can be delivered to the organ or tumor *via* the nanoprodrug strategy, it is still difficult to produce a satisfactory therapeutic effect by administration of a single type of drug for cancer treatment.[27–29] Therefore, the development of an effective platform for controlled combination drug therapy has received wide attention as a new approach to antitumor treatment.[30–35]

Podophyllotoxin is an important anticancer lead compound isolated from the *Podophyllum* genus. Using podophyllotoxin as a starting compound, a large number of derivatives have been synthesized, which include two anticancer drugs etoposide (VP16) and teniposide (VM26).[36–38] However, the overwhelming majority of podophyllotoxin-derived active compounds were gradually abandoned. 4′-*O*-Demethyl-4β-(4″-aminoanilino)-4-desoxy-podophyllotoxin (**AdP**) is one of the phenylamino-containing podophyllotoxin derivatives which was first reported in 1990.[39] This compound exhibits better DNA topoisomerase II inhibitory activity than its structural analogue GL331, a podophyllotoxin-derived candidate anticancer drug, but no in-depth research has been reported.[40,41] Therefore, we proposed a novel nanoprodrug system in which the readily available podophyllotoxin natural products are connected with methoxy polyethylene glycol (mPEG) *via* a multifunctional azobenzene group. The resulting amphiphilic prodrug can effectively improve the water solubility of podophyllotoxin by forming nanosized micelles. As a consequence of the cleavage of the azo bond in the presence of azoreductases, active **AdP** will be *in situ* generated in the colon, in which a phenylamino group could be modified on the parent compound (Scheme 1). Furthermore, the colon-targeted nanoprodrug can be used as a building block to construct a biocompatible supramolecular hydrogel for loading another water-soluble anticancer drug just by introducing α-CD to the system (Scheme 1). The strong hydrogen bonding interaction among adjacent α-CD pseudopolyrotaxanes (PPRs) provides a shell–shell interaction for driving the self-assembly of the prodrug nanomicelles into a supramolecular hydrogel.[42] Combination of the colon-targeted podophyllotoxin nanoprodrug and its hydrogel form provides a new strategy to reuse bioactive natural products and offers a powerful carrier for co-delivery of hydrophobic and hydrophilic drugs for drug combination.

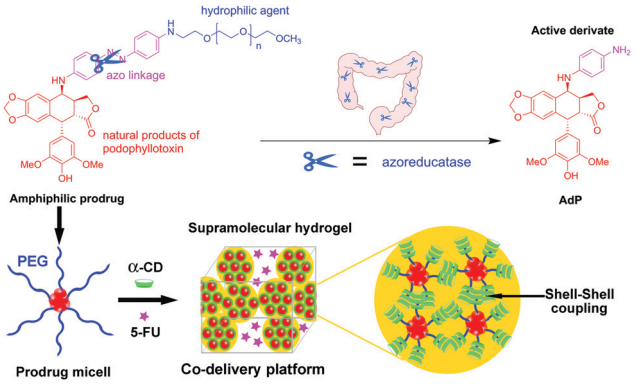

Scheme 1 Schematic illustration of the design of the azo-based podophyllotoxin nanoprodrug and its hydrogel form for drug combination.

Experimental

The synthesis route to the azo-based podophyllotoxin prodrug is shown in Fig. 1a.

Synthesis of compound 2[43]

In brief, a solution of podophyllotoxin natural products 4′-*O*-demethylepipodophyllotoxin (compound **1a**, 2.5 mmol) or podophyllotoxin (compound **1b**, 2.5 mmol) in 25 mL of dry CH_2Cl_2 was bubbled with HBr gas at 0 °C for 45 min. The unreacted HBr was removed through bubbling with N_2 and the solution was evaporated to obtain the crude intermediate compounds.

The intermediate compounds (1 mmol) were dissolved in dry CH_2Cl_2 (10 mL), and K_2CO_3 (3 mmol, 414 mg) was added under a N_2 atmosphere. 5 min later, 4,4′-azodianiline (1.2 mmol, 254 mg) was added and allowed to react for 4 h. The reaction solution was filtered, evaporated and purified to obtain compound **2** as a gray solid (53–61%). Compound **2a**, ^{1}H NMR (400 MHz, d_6-DMSO) δ: 3.05–3.08 (m, 1H, 3-H), 3.28–3.36 (dd, 1H, J = 5.2 Hz, 14.4 Hz, 2-H), 3.66 (br, 6H, 3′,5′-OCH_3), 3.70 (m, 1H, 11-H), 4.39 (t, 1H, J = 7.6 Hz, 11-H), 4.54 (d, 1H, J = 5.2 Hz, 1-H), 4.98 (m, 1H, 4-H), 6.01 (d, J = 10.4 Hz, 2H, 13-H), 6.29 (s, 2H, 2′,6′-H), 6.57 (s, 1H, 8-H), 6.64 (d, 2H, J = 8.8 Hz, 8″,12″-H), 6.82 (m, 3H, 5,3″,5″-H), 7.56 (d, 2H, J = 8.4 Hz, 9″,11″-H), 7.62 (d, 2H, J = 8.4 Hz, 2″,6″-H); ^{13}C NMR (100 MHz, d_6-DMSO) δ: 175.1, 151.6, 150.5, 147.7, 147.6, 147.6, 147.0, 144.0, 143.6, 135.2, 132.3, 131.4, 130.7, 124.4, 124.3, 113.9, 109.9, 109.7, 109.0, 101.7, 68.9, 60.2, 56.5, 50.8, 43.3, 41.4, 38.7; HRMS: $C_{33}H_{30}N_4O_7Na$ for $[M + Na]^+$, calculated 617.2007, found 617.2014. Compound **2b**, ^{1}H NMR (400 MHz, $CDCl_3$) δ: 3.05–3.06 (m, 1H, 3-H), 3.11–3.16 (dd, 1H, J = 4.7 Hz, 12.0 Hz, 2-H), 3.77 (br, 6H, 3′,5′-OCH_3), 3.82 (s, 3H, 4′-OCH_3), 4.00 (t, 1H, J = 9.6 Hz, 11-H), 4.42 (t, 1H, J = 7.9 Hz, 11-H), 4.62 (d, 1H, J = 4.6 Hz, 1-H), 4.79 (m, 1H, 4-H), 5.97 (d, 2H, J = 6.8 Hz, H-13), 6.33 (s, 2H, 2′,6′-H), 6.54 (s, 1H, 8-H), 6.63 (d, 2H, J = 8.2 Hz, 8″,12″-H), 6.74 (d, 2H, J = 7.8 Hz, 3″,5″-H), 6.81 (s, 1H, 5-H), 7.75 (d, 2H, J = 7.7 Hz, 9″,11″-H), 7.80 (d, 2H, J = 8.0 Hz, 2″,6″-H); ^{13}C NMR (100 MHz, $CDCl_3$) δ: 174.5, 152.6, 148.8, 148.7, 148.4, 147.7, 145.6, 135.0, 131.9, 130.0, 124.6, 124.5, 114.8, 112.1, 109.9, 109.3, 108.3, 101.6, 68.8, 60.8, 56.3, 52.4, 43.6, 41.8, 38.7; HRMS: $C_{32}H_{29}N_4O_7$ for $[M + H]^+$, calculated 609.2344, found 609.2335.

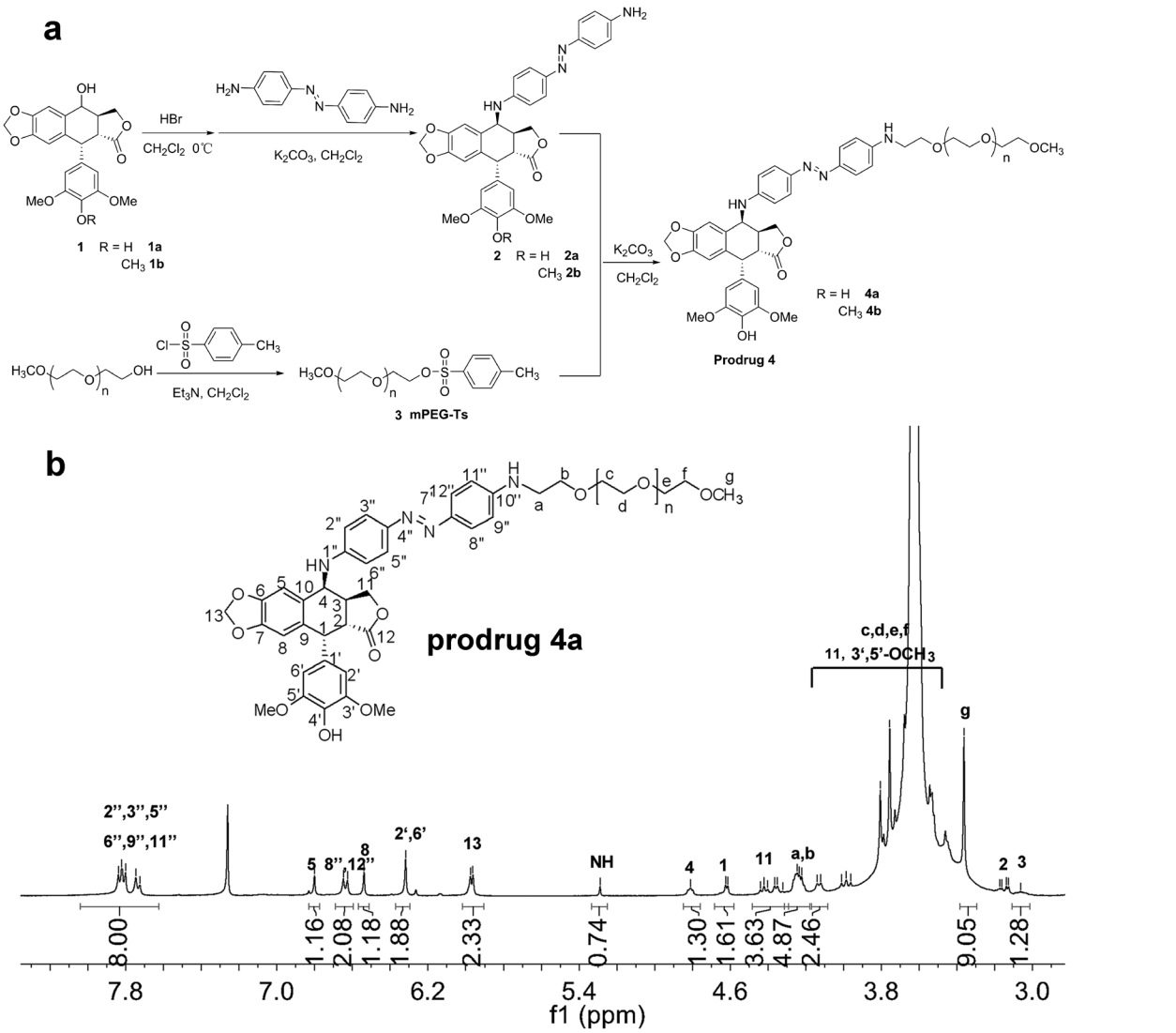

Fig. 1 Synthetic routes to the azoreductase-responsive amphiphilic prodrug (a). ^{1}H NMR of prodrug **4a** (b) in $CDCl_3$.

Synthesis of mPEG-Ts (compound 3)

In brief, to a solution of monomethoxy polyethylene glycol (mPEG, M_w = 1900, 2.63 mmol, 5.0 g) in CH_2Cl_2 (10 mL), triethylamine (7.89 mmol, 1.11 mL) was added. After being stirred under a N_2 atmosphere for 5 min, p-toluenesulfonyl chloride (5.26 mmol, 1.0 g) was added and allowed to react for 4 h. The crude product was purified using a dextran gel column to obtain intermediate **mPEG-Ts** (4.5 g, compound **3**). ^{1}H NMR (400 MHz, $CDCl_3$) δ: 7.75 (d, 2H, J = 8.2 Hz, 2, 6-H), 7.30 (d, 2H, J = 8.0 Hz, 3, 5-H), 4.11–4.13 (m, 2H, 8-H), 3.50–3.77 (m, 9,10,11-H), 3.34 (s, 3H, H-12), 2.41 (s, 3H, H-7).

Synthesis of the azo-based podophyllotoxin prodrug (compound 4)

The compound **2** (1 mmol) was dissolved in dry CH_2Cl_2 (10 mL), and K_2CO_3 (3 mmol, 414 mg) was added under a N_2 atmosphere. 5 min later, **mPEG-Ts** (1.5 mmol, 3.1 g) was added and allowed to react for 24 h. The reaction solution was filtered, evaporated and purified using a dextran gel column to obtain the prodrug. Compound **4a**, ^{1}H NMR (400 MHz, $CDCl_3$) δ: 7.72–7.84 (m, 6H,2″,3″,5″,6″,9″,11″-H), 7.72–7.74 (8'', 12''-H), 6.80 (s, 1H, 5-H), 6.63–6.65 (d, 2H, J = 8.8 Hz, 8″,12″-H), 6.54 (s, 1H, 8-H), 6.32 (s, 2H, 2′,6′-H), 5.96 (s, 1H, 13-H), 5.98 (s, 1H, 13-H), 5.29 (s, NH), 4.81 (m, 1H, 4-H), 4.61 (d, 1H, J = 4.6 Hz, 1-H), 4.42 (t, 1H, J = 7.7 Hz, 11-H), 4.23 (m, 4H, -NH-CH_2CH_2O- of PEG chain), 3.46–4.01 (m, 11, 3′,5′-OCH_3, –OCH_2CH_2O- units of PEG chain), 3.36 (s, 3H, –OCH_3 of PEG chain), 3.28–3.36 (dd, 1H, J = 4.6 Hz, 14.0 Hz, 2-H), 3.06 (m, 1H, 3-H); ^{13}C NMR (100 MHz, $CDCl_3$) δ: 174.6, 152.9, 150.3, 148.3, 147.8, 147.6, 146.5, 146.4, 144.8, 134.2, 132.0, 130.5, 130.1, 124.5, 124.4, 112.5, 112.1, 109.9, 109.3, 108.0, 101.6, 71.9, 71.3, 70.5, 70.3, 69.4, 68.8, 59.0, 56.5, 56.3, 56.0, 52.3, 43.4, 43.2, 42.7, 41.9, 38.6. Compound **4b**, ^{1}H NMR (400MHz, $CDCl_3$) δ: 7.83 (m, 6H, 2″,3″,5″,6″,9″,11″-H), 7.75 (8″,12″-H), 6.80 (s, 1H, 5-H), 6.64 (d, 2H, 8″, 12″-H), 6.54 (s, 1H, 8-H), 6.32 (s, 2H, 2′,6′-H), 5.98 (s, 1H, 13-H), 5.98 (s, 1H, 13-H), 5.29 (s, NH), 4.81 (m, 1H, 4-H), 4.62 (1H, 1-H), 4.42 (1H, 11-H), 4.26 (m, 4H, –NH–CH_2CH_2O- of

PEG chain), 3.46–3.99 (m, 11, 3′,4′,5′-OCH_3, –OCH_2CH_2O- units of PEG chain), 3.36 (s, 3H, –OCH_3 of PEG chain), 3.13 (dd, 1H, 2-H), 3.06 (m, 1H, 3-H); ^{13}C NMR (100 MHz, $CDCl_3$) δ: 174.4, 152.6, 149.4, 148.8, 148.4, 147.7, 146.2, 146.0, 145.5, 144.2, 137.3, 131.9, 129.8, 125.1, 123.3, 119.6, 114.9, 112.0, 110.0, 109.2, 108.3, 101.6, 71.9, 70.5, 70.3, 68.9, 63.6, 60.7, 59.0, 56.3, 52.3, 43.6, 41.8, 38.6, 32.1.

Degradation selectivity of the prodrug

To the solution of prodrug **4a** in deoxygenated PBS buffer (pH = 7.4, 10 mM, 2 mL), 1 mL of PBS solution, proteinase K solution, lipase solution (10 mg mL^{-1}), $Na_2S_2O_4$ solution (10 mg mL^{-1}) and rat cecal content solution were added by bubbling nitrogen, respectively. The mixture was incubated for 12 h at 37 °C and detected by HPLC or UPLC-MS/MS to monitor the degradation of the prodrug and the release of **AdP**.

Preparation of a nanoprodrug based supramolecular hydrogel

The colon-targeted nanoprodrug was further used as a building block to interact with α-CD for preparing a supramolecular hydrogel according to our previously reported method.[42] The concentration of the prodrug was fixed at 20 mg mL^{-1} and the concentration of α-CD ranged from 40 to 120 mg mL^{-1}. The lyophilized supramolecular hydrogels were analysed by scanning electron microscopy (SEM) and X-ray diffraction (XRD). The 5-FU loaded nanoprodrug hydrogel was obtained with the same approach just by mixing 5-FU (2 mg mL^{-1}) with the prodrug solution before introducing α-CD to the mixture.

Imaging mass spectrometry (IMS) analysis

Normal diet mice were sacrificed after gavage with the prodrug (compound **4b**) hydrogel (0.1 mL, 100 mg kg^{-1}) for 16 h; different organs were dissected and frozen at −80 °C. As a control, cecal and colorectal tissues of mice were also dissected after gavage with PBS (0.1 mL) at 16 h. The frozen tissues were fixed on a holder and sliced at 20 μm thickness at −20 °C using a cryomicrotome. The tissue sections were placed on ITO-coated glass slides (sheet resistivity ≤5 Ω, Shenzhen, China). The glass slides were dried and the surface was deposited with matrix CHCA using an iMLayer (Shimadzu, Kyoto, Japan).

IMS analysis was performed using an imaging mass spectrometer (iMScope TRIO Shimadzu, Kyoto, Japan). Positive-ion detection mode (m/z range of 200–650) was used in MS and MS/MS analysis, respectively. The target compound was confirmed with selected fragment ion m/z 397.13 in MS/MS analysis.

In vitro drug release

A cuvette containing 1 mL of 5-FU loaded nanoprodrug hydrogel was immersed in 30.0 mL of PBS (pH 7.4), PBS containing 10 mg mL^{-1} $Na_2S_2O_4$ or PBS containing 10 mg mL^{-1} amylase in a 37 °C water bath, respectively. At predetermined time intervals, 5 mL of release medium was changed. The concentrations of 5-FU, prodrug **4a** and **AdP** released from hydrogels were determined by HPLC. In the second stage, 4 mg of prodrug **4a** was dissolved in 10 mL of deoxygenated PBS buffer, and then 10 mL of rat cecal content solution were added by bubbling nitrogen and incubated for 12 h at 37 °C. At predetermined time intervals, 2.0 mL of release medium was removed and analysed by UPLC-MS/MS to determine the concentrations of the **AdP** released from prodrug **4a**.

In vitro cytotoxicity assays

AdP, prodrug **4a**, 5-FU and a mixture of **AdP**/5-FU with 1 : 1 mole ratio were used to evaluate the *in vitro* cytotoxicity against HepG2 cells. Hep G2 cells were incubated with 0, 3.13, 6.25, 12.50, 25.00, 50.00 and 100.00 μM of test compounds for 72 h and MTT assay was performed to determine the cell viability according to the reported method.[44] The CI values with the combination use of **AdP** and 5-FU (ESI,† Tables S1 and S2) were calculated by the computerized Chou-Talalay method.[45,46]

Results and discussion

Synthesis and characterization of the nanoprodrug

Podophyllotoxin natural product compounds **1a** and **b** are the main secondary metabolites isolated from the *Podophyllum* genus. As shown in Fig. 1a, these two readily available natural compounds were used as a starting compound and further connected with an azobenzene linker, 4,4′-azodianiline, to afford an important podophyllotoxin-derived intermediate (compounds **2**) bearing an azo bond. Then, the target azoreductase-responsive amphiphilic prodrug (prodrug 4) was prepared by the reaction of compounds **2** with **mPEG-Ts** (M_n = 1900). The structures of the intermediate products were confirmed using ^{1}H and ^{13}C NMR spectra (Fig. S1–S6, ESI†). The chemical structures of the prodrug were confirmed by ^{1}H NMR (see Fig. 1b for prodrug **4a** and Fig. S7 (ESI†) for prodrug **4b**) and ^{13}C NMR (Fig. S8 and S9, ESI†). Taking prodrug **4a** as an example, besides the characteristic H signals that belong to the molecular framework of podophyllotoxin, the signals of H-2″,3″,5″,6″,8″,9″,10″, and 11″ belonging to the azobenzene linker and H signals of a–g in the PEG chain can be clearly observed in ^{1}H NMR spectra (Fig. 1b), which indicated that the ingeniously designed prodrug has been successfully synthesized. It should be noted that colon tissue contains a large number of azoreductases specifically expressed by colonic microflora, which can selectively reduce the azobenzene linker to form the corresponding aniline group. Therefore, as a consequence of the cleavage of the azobenzene linker in the prodrug reduced by azoreductase, one of the corresponding aniline groups will be retained on the parent molecular structure to *in situ* form the target compound **AdP** (Scheme 1).

Due to the poor water solubility of parent podophyllotoxin molecules, the resultant amphiphilic prodrug will aggregate in water to form typical nanomicelles (Fig. 2a), in which the hydrophobic precursor molecule and hydrophilic PEG chains are located in the core and surface of nanomicelles *via* the azo linkage. It should be noted that the loading efficiency of active **AdP** in the nanoprodrug is constant, which is conducive to regulating the proportion of the drug for combination therapy.

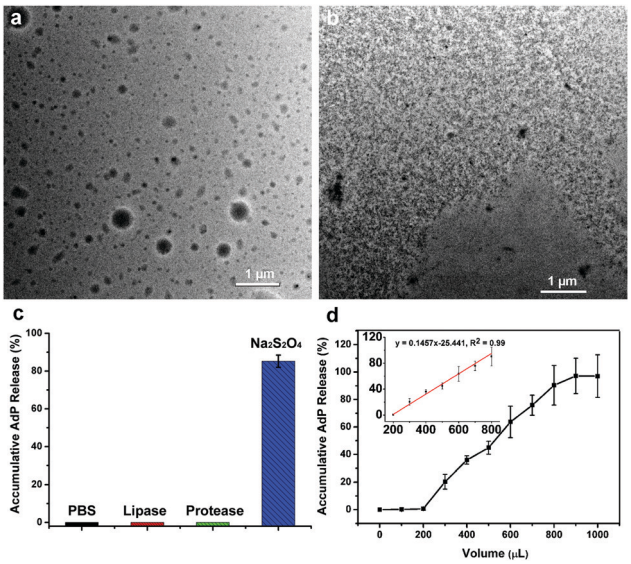

Fig. 2 The TEM images of prodrug 4 micelle solution before (a) and after (b) introducing 10 mg mL^{-1} $Na_2S_2O_4$ to the solution. (c) Accumulative release of **AdP** from prodrug **4a** toward PBS, lipase, protease and $Na_2S_2O_4$. (d) The release behavior of **AdP** upon addition of different volumes of rat cecal contents.

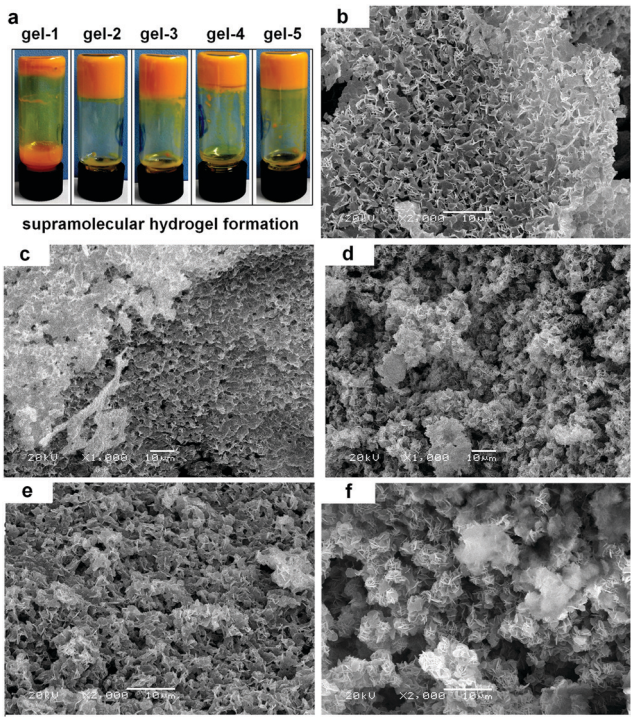

Fig. 3 (a) Photos of the supramolecular hydrogels made of prodrug 4 nanomicelles and different amounts of α-CD. For gels 1–5, the concentrations of α-CD are 40, 60, 80, 100 and 120 mg mL^{-1}, respectively. (b–f) are SEM images corresponding to gels 1–5, respectively.

The activation of **AdP** from the prodrug was investigated by HPLC upon addition of an alternative to azoreductase (sodium dithionite, $Na_2S_2O_4$), and other common enzymes in the digestive system, such as proteinase and lipase. Remarkable **AdP** release was only observed when prodrug **4a** reacted with $Na_2S_2O_4$ while no notable change in the distinct peak of the prodrug **4a** was observed in the presence of digestive enzymes (Fig. 2c and Fig. S10, ESI†). Meanwhile, the TEM images of prodrug 4 nanomicelle solution after introducing $Na_2S_2O_4$ indicated that the micelle structures were totally disrupted (Fig. 2b). Furthermore, the activation of **AdP** from prodrug **4a** was investigated by UPLC-MS/MS upon addition of different amounts of rat cecal contents. The amount of released **AdP** was also determined by UPLC-MS/MS using the equation for the calibration curve (Fig. S11, ESI†). When the volume of rat cecal content solution was increased from 200 μL to 900 μL, the accumulated release of **AdP** from prodrug **4a** reached above 95% at an almost constant rate (Fig. 2d). This result can be ascribed to the fact that there were a large number of azoreductases present in rat cecal contents.[47–49] Therefore, we can conclude that the target **AdP** molecules can be released in the colon from the proposed nanoprodrug with high selectivity.

Progressive self-assembly of the prodrug micelles

Our previously reported work has proved that PEGylated amphiphilic prodrug nanomicelles can be used as a building block to further construct superstructures, such as supramolecular hydrogels, with the introduction of α-CD.[42,50,51] The strong hydrogen bonding interaction among adjacent pseudopolyrotaxanes (PPRs), formed between α-CD and PEG chains distributed on the micellar surface, will provide a so-called shell–shell coupling effect to drive the prodrug nanomicelles to further aggregate and self-assemble into a supramolecular hydrogel. The resulting supramolecular hydrogel not only has the advantages of prodrug nanomicelles, but also increases the space and dimensions of the micelle system during the progressive self-assembly process, which makes it possible to load other antitumor drugs, especially water-soluble antitumor drugs. Therefore, to satisfy the demand of drug carriers for combination therapy in clinics,[27–29] different amounts of α-CD were introduced into prodrug 4 micelle solution (20 mg mL^{-1}). A turbid solution was observed when the concentrations of α-CD ranged from 40 to 120 mg mL^{-1}, and stable hydrogels can be obtained at a wide range of α-CD concentrations (Fig. 3a), even as low as 60 mg mL^{-1}. The threading and dethreading of α-CD from the PEG chain is a dynamic equilibrium process in typical PPR formation. At relatively lower concentration of α-CD, it tends to dethread from both ends of the PEG chain side.[52] In this PEGylated prodrug nanomicelle system, the PEG brushes on the micellar surface can provide only one chain end, which is beneficial for retaining α-CD in the PPR structure. With increasing the concentration of α-CD, the hydrogel formation time is dramatically reduced. When the concentration is above 100 mg mL^{-1}, the hydrogel can be rapidly formed during the ultrasonication process. The lyophilized samples were further observed by SEM to investigate the progressive self-assembly process after adding different amounts of α-CD (Fig. 3b–f). With increasing the amount of α-CD, the inner morphology of the prodrug/α-CD complex changes from typical lamellar

aggregates to a unique morphology piled up with porous microspheres. This can be interpreted as the strengthened shell–shell interaction among prodrug nanomicelles with the increased number of PPRs in this system. Lower concentration of α-CD generated relatively few PPRs on the prodrug micellar surface and can only provide weak shell–shell interaction, resulting in a morphology similar to typical pure PPR supramolecular structures. However, at increasing concentrations (above 80 mg mL^{-1}), sufficient PPRs could be formed and retained onto the micellar surface. The strong hydrogen bonds among adjacent PPRs provide an enhanced shell–shell interaction to induce PPR-modified prodrug micelle self-assembly into porous microspheres. Finally, the interactions among adjacent microspheres provide the necessary cross-links and building blocks for supramolecular hydrogel formation (Fig. 4a). All freeze-dried prodrug/α-CD complexes were further analysed using complementary X-ray diffraction (XRD) to confirm the formation of the PPR structure in self-assembled hydrogels. In the patterns of all five gels (Fig. 4b), newly generated diffraction peaks (around 2θ = 19.9° and 22.6°) belonging to the (210) and (300) planes of crystalline columnar α-CD that originated from α-CD PPRs were observed.[53,54] Meanwhile, the peaks (2θ = 19.1° and 23.2°) belonging to the prodrug disappeared in the pattern of gels 2–5, implying that

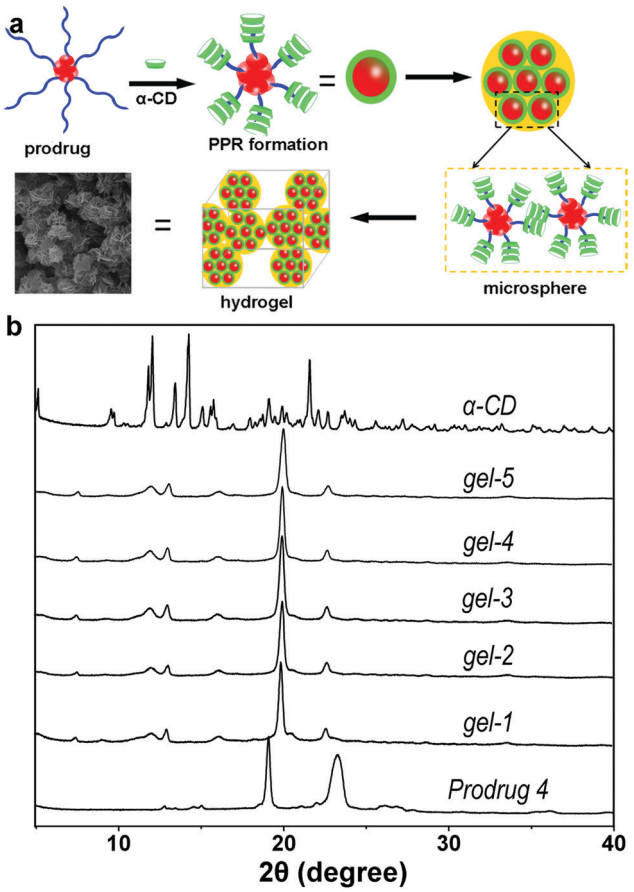

Fig. 4 (a) Schematic representation of the process of hydrogel formation. (b) XRD patterns for freeze-dried gels 1–5, prodrug **4a** and α-CD.

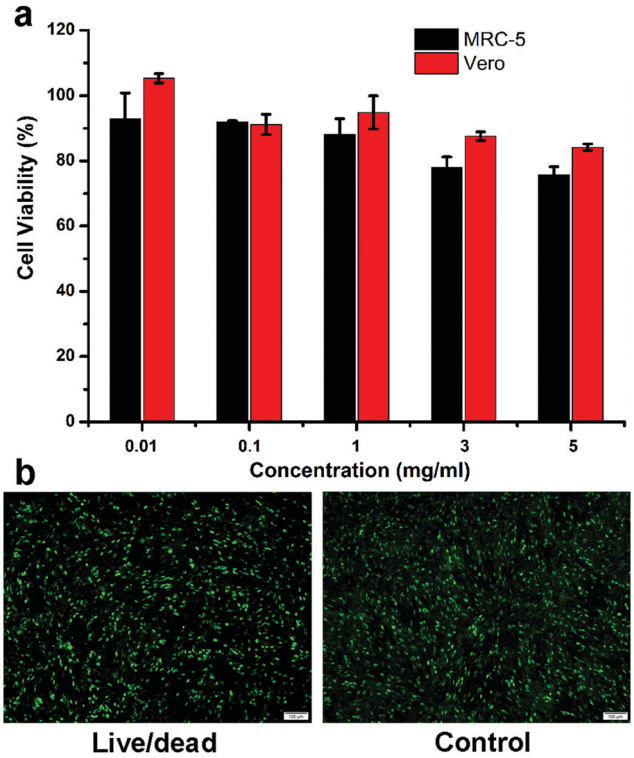

Fig. 5 (a) The cell viability of the prodrug hydrogel using MTT assay. (b) Live/dead assay of Vero cells incubated with the prodrug/α-CD hydrogel (1 mg mL^{-1}) for 24 h. All scale bars: 100 μm. Red and green colours represent dead and live cells.

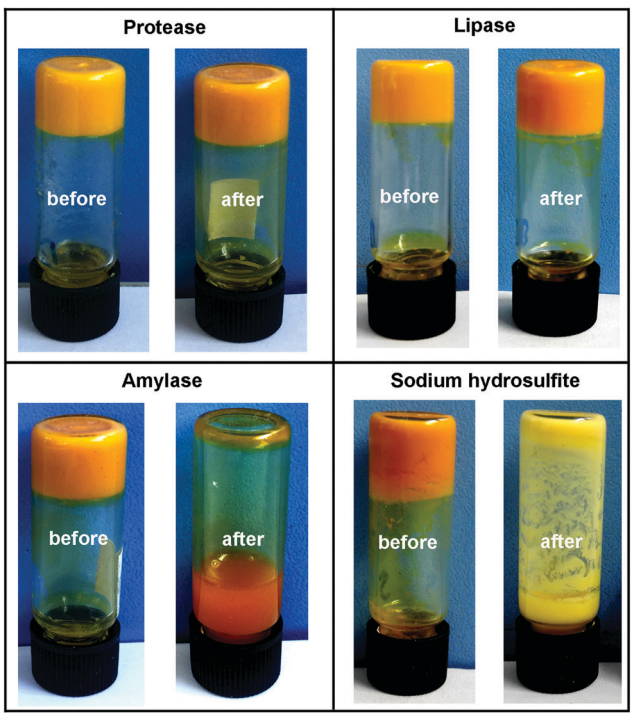

Fig. 6 Optical photos of the nanoprodrug **4a** hydrogels before and after introducing protease, lipase, amylase and sodium hydrosulfite.

most of the PEG chains participated in the PPR formation. The diffraction peak around 2θ = 23.2° belonging to the prodrug was still found in the pattern of gel-1, which indicates that relatively few PPRs were formed at low concentration of α-CD. These results confirm that the introduction of α-CD into PEGylated prodrug micelles can generate PPR suprastructures, which effectively induce the aggregation of prodrug micelles and make the formation of a hydrogel possible.

It has been extensively proved that cyclodextrin PPR hydrogels have significant biocompatibility, but the cytotoxicity of PPR hydrogels incorporated with an azo linked prodrug have not yet been verified. Human embryonic lung fibroblast cells (MRC-5) and kidney cells of African green monkey (Vero) were used to evaluate the biocompatibility by MTT assay first (Fig. 5a). The cell viability of both two cell lines against the prodrug hydrogel is higher than 90% after incubation for 3 days, even at a high concentration (1.0 mg mL^{-1}). To further visualize the cell viability on the prodrug hydrogel, live/dead assay was performed using Vero cells. As shown in Fig. 5b, after incubation with both prodrug hydrogel and PBS (control) for 24 h (Fig. 5b), the fluorescence images showed almost no red color in both groups. These results indicate that there are almost no cytotoxic effects of the PEGylated podophyllotoxin nanoprodrug and its hydrogel form, which is beneficial for colon-specific drug delivery.

The response performance of the prodrug hydrogel was investigated upon addition of $Na_2S_2O_4$, lipase, proteinase and amylase. As shown in Fig. 6, the hydrogel form showed almost

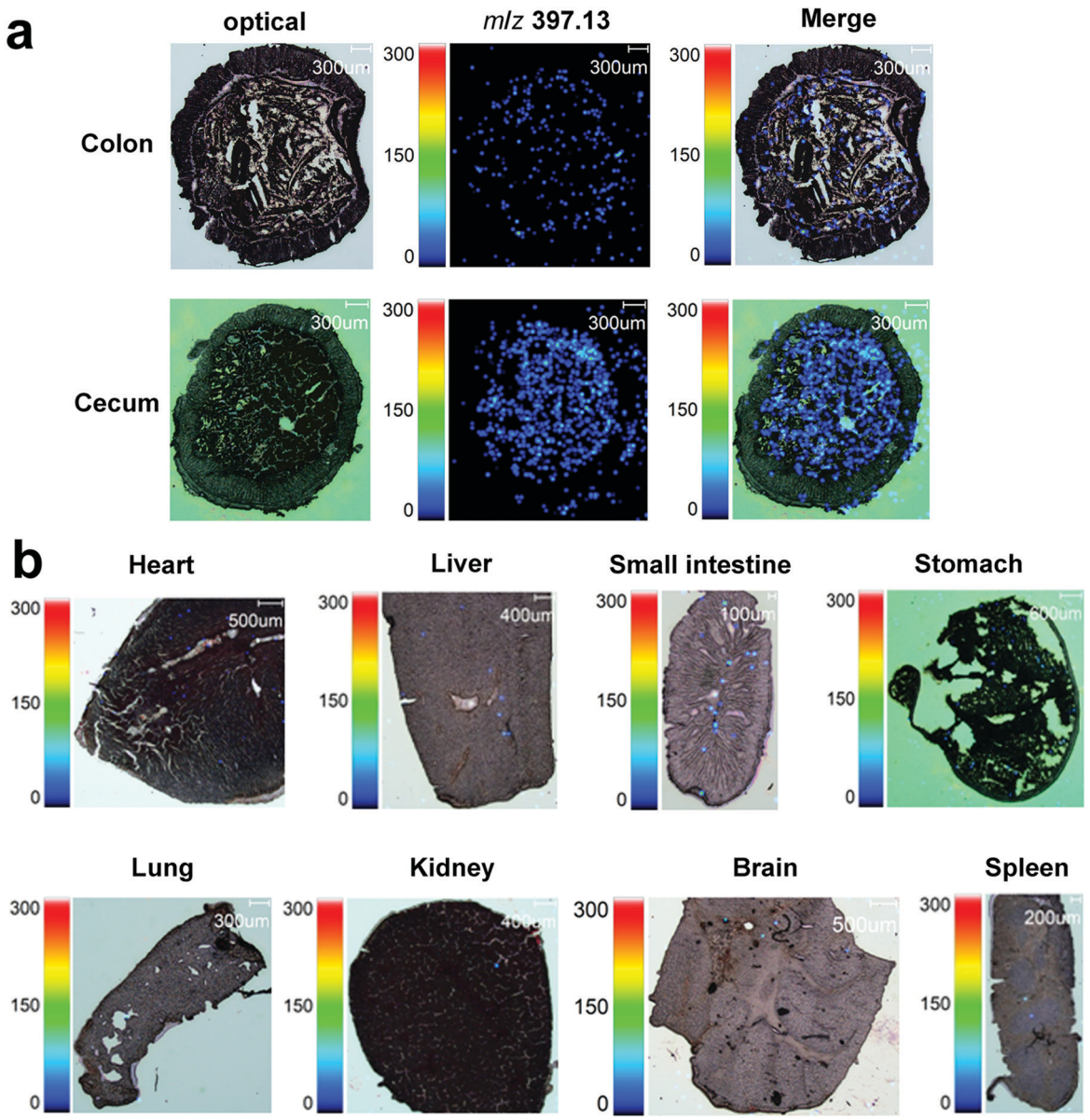

Fig. 7 IMS of tissue sections at 16 h after gavage with the prodrug **4b** hydrogel in mice. (a) Optical, IMS, and merged images of podophyllotoxin derivatives in colon and cecal tissue. (b) Merged images of other organs.

no change after incubation with lipase and proteinase for 30 min. However, it showed a typical gel–sol transition behavior after incubation with amylase and $Na_2S_2O_4$. It could be ascribed to the fact that the degradation of α-CD in the presence of amylase can destroy the PPR structure, resulting in the dissociation of the supramolecular hydrogel further. It should be noted that the abundant colonic microflora can secrete corresponding enzymes, such as amylase, which are only active in the colon on degradation of polysaccharides.[55–57] Furthermore, the breakage of the azo linkage in prodrug upon addition of $Na_2S_2O_4$ can destroy the micelle structure and supra-cross links, and lead to destruction of supramolecular hydrogel. Therefore, through the combination use of amylase and azoreductase which are specifically secreted by colonic microflora, the proposed prodrug hydrogel shows significant potential in co-delivering active natural products and other water soluble drugs to the colon for combination therapy purpose.

Although the enzyme-responsive drug release and gel–sol transition behavior of the azo linked prodrug and its hydrogel form have been proved *in vitro*, the colon-specific delivery of podophyllotoxin natural products *in vivo* still needs to be further verified. Therefore, IMS was performed in mouse tissue after intragastric administration of the prodrug **4b** hydrogel to map the biodistribution of released molecules precisely. As a control, IMS analysis was also carried out after intragastric administration of the same volume of PBS. In the first order spectra of molecules released from prodrug **4b** after the reduction of the azo bond, the quasimolecular ion at *m*/*z* 505.19 $[M + H]^+$ (Fig. S12b, ESI†) afforded a characteristic fragment ion $[M\text{-ursol} + H]^+$ in MS/MS experiments (Fig. S12c, ESI†), which corresponded to the loss of ursol from the ion $[M + H]^+$ under a H transfer mechanism (Fig. S12a, ESI†).[58,59] Therefore, the quasimolecular ion, *m*/*z* 505.19, was selected as the precursor ion in MS/MS analysis and the fragment ion *m*/*z* 397.13 was chosen as the diagnostic ion for evaluating the biodistribution of released podophyllotoxin derivatives in different tissue sections. Fig. 7 presents the biodistribution of podophyllotoxin derivatives (MS/MS fragmentation, *m*/*z* 397.13) from the prodrug **4b** hydrogel in different organs. As seen in Fig. 7a, the diagnostic ion belonging to target compounds (*m*/*z* 397.13) was observed clearly in colon and cecal tissue sections. However, in the control group, few characteristic MS signals were found in colon and cecal tissue sections (Fig. S13, ESI†). Meanwhile, in other organs, almost no characteristic MS signals were found (Fig. 7b). These results presented *in vivo* evidence at the molecular level that the prodrug and its hydrogel form possess excellent ability to release podophyllotoxin derivatives in the colon in a targeted manner.

Encouraged by the above results, the prodrug hydrogel was further used as a carrier to load another hydrophilic anti-cancer drug during the progressive self-assembly process. 5-FU is a typical water-soluble drug with a different anticancer mechanism from the podophyllotoxin drug. The release behavior of 5-FU, the prodrug and **AdP** from the hydrogel was investigated under different conditions. In a normal physiological environment (PBS, pH 7.4), the 5-FU loaded hydrogel presented a sustained release of 5-FU, and a relatively small amount of prodrug **4a**, but no **AdP** can be detected during the entire release process (Fig. 8a). This result indicated that the azo-linked prodrug and its hydrogel form are stable in a normal physiological environment. The release rate of both 5-FU and prodrug was significantly accelerated (Fig. 8b) in the presence of amylase, which is mainly because of the partial gel–sol transition of the prodrug hydrogel on the contact surface induced by the degradation of α-CD. Similarly, no **AdP** was found in the presence of amylase. In the next stage, the released prodrug **4a** can also continue to release active **AdP** due to the breakage of the azo linkage in the presence of rat caecal contents (Fig. 8c). When $Na_2S_2O_4$ was introduced into the 5-FU loaded hydrogel, the release of both 5-FU and **AdP** was observed, resulting from the disruption of prodrug nanomicelles (Fig. 8d). Meanwhile, the dramatically accelerated release of 5-FU is also directly attributable to the disruption of prodrug nanomicelles which is essential for maintaining the structural stability of the hydrogel. These results suggest that the enzymes specifically secreted by the colon can effectively accelerate the release rate of 5-FU and targeted delivery of **AdP** to the colon from the prodrug hydrogel, which is beneficial for combination therapy in the treatment of colon-related diseases.

Finally, the cytotoxicity of **AdP**, 5-FU and the combination of 5-FU and **AdP** against Hep G2 cells was investigated using MTT assay to evaluate the combination effect of **AdP** and 5-FU. In addition, the cytotoxicity of prodrug **4a** was also investigated. As shown in Fig. S14 (ESI†), the prodrug exhibited weak cytotoxic activity against normal cell lines, normal human liver L-02 and mouse myoblast C2C12 cells. Moreover, prodrug **4a** presented less cytotoxicity than **AdP** for Hep G2 cells in the entire range of concentrations (Fig. 9a), indicating that the resultant prodrug can effectively release **AdP** to the colon on the basis of reducing its toxicity in the delivery process. Furthermore, the combination use of **AdP** and 5-FU showed enhanced cytotoxicity compared to single drug treatment.

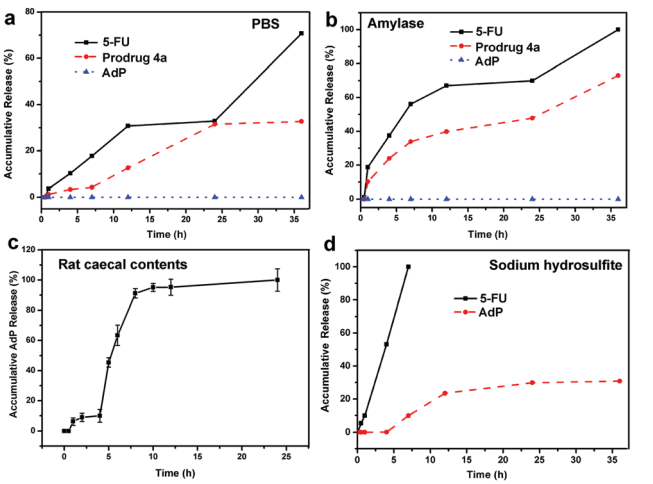

Fig. 8 Release kinetics of 5-FU, prodrug **4a** and **AdP** from the 5-FU loaded prodrug hydrogel in PBS (a), in the presence of 10 mg mL^{-1} amylase (b) or $Na_2S_2O_4$ (d). (c) **AdP** release kinetics from prodrug **4a** in the presence of rat cecal contents.

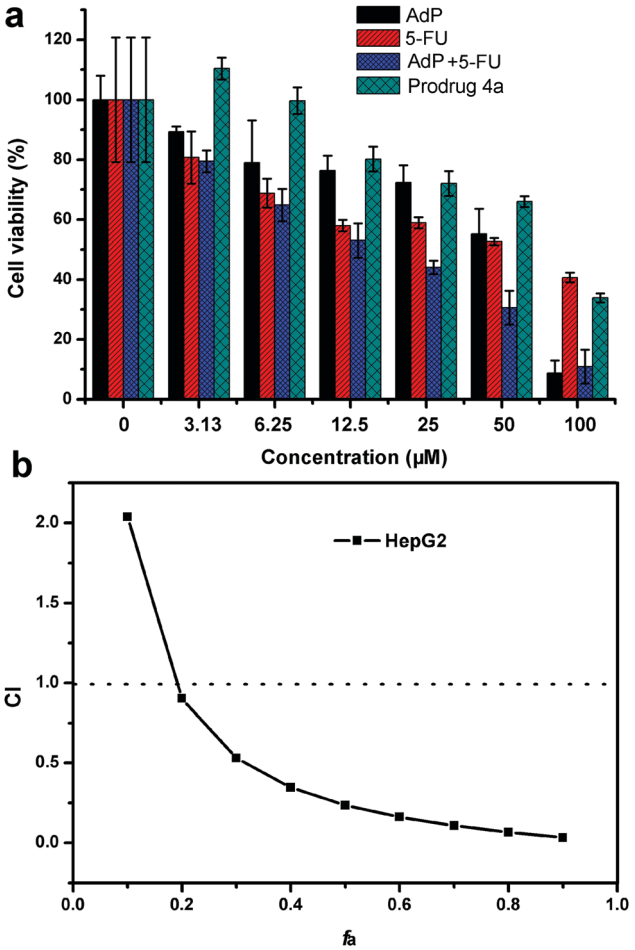

Fig. 9 (a) *In vitro* cytotoxicity results against Hep G2 cells determined by MTT assay. (b) CI value *versus* f_a.

The combination index (CI) of **AdP** and 5-FU was further calculated according to the Chou-Talalay method (Tables S1 and S2, ESI†).[45,46] As seen in Fig. 9b, the CI was <1 for Hep G2 cells at $\geq f_a20$, demonstrating a significant synergistic interaction between the two drugs. These results implied that the proposed prodrug can effectively reduce the toxicity of **AdP** and its hydrogel form provides a possibility to enhance the therapeutic effect of **AdP** by loading another drug.

Conclusions

In conclusion, taking an important anticancer natural product podophyllotoxin as a proof of concept, a new-type of azo-based, amphiphilic, and colon-targeted podophyllotoxin-derived nanoprodrug was designed and synthesized. The readily available podophyllotoxin natural products were used as starting compounds to connect with PEG chains *via* a multifunctional azobenzene group, and highly selectively activated by azoreductase, which resulted in the generation of active podophyllotoxin derivatives in the colon through an ingenious *in situ* modification strategy. Subsequently, host–guest inclusion based self-assembly was performed to generate a supramolecular hydrogel. The capability to deliver active podophyllotoxin derivatives to the colon based on the resultant nanoprodrug and its hydrogel form has been successfully demonstrated by investigating the release behavior in the presence of a chemical mimic of azoreductase, digestive enzymes, rat cecal contents, and the biodistribution of podophyllotoxin derivatives in mouse tissue was also precisely mapped at the molecular level using IMS. Furthermore, the hydrogel form of the podophyllotoxin-derived prodrug provides an effective platform to load another water-soluble anticancer drug, 5-FU, for combination therapy. *In vitro* assays demonstrated that the combination use of 5-FU and podophyllotoxin derivatives produces significant synergetic cytotoxicity to cancer cells. We believe that the colon-targeted prodrug obtained from natural products and its hydrogel form will not only provide an attractive strategy for reconsideration of bioactive natural products and their derivatives, but also provide an effective platform for co-delivery of multiple drugs for drug combination. However, for colon tumor site-specific delivery of these anticancer natural products, the ligand-mediated targeted strategy needs to be considered further in a tumor-bearing animal model.

Conflicts of interest

There are no conflicts to declare.

Acknowledgements

This work was supported by the National Natural Science Foundation of China (No. 21974145), and the Scholar Program of West Light Project, Youth Innovation Promotion Association of the Chinese Academy of Sciences (2017457).

References

1 T. Rodrigues, D. Reker, P. Schneider and G. Schneider, *Nat. Chem.*, 2016, **8**, 531.
2 A. L. Harvey, R. A. Edrada-Ebel and R. J. Quinn, *Nat. Rev. Drug Discovery*, 2015, **14**, 111.
3 B. A. Shen, *Cell*, 2015, **163**, 1297.
4 E. Patridge, P. Gareiss, M. S. Kinch and D. Hoyer, *Drug Discovery Today*, 2015, **21**, 204.
5 J. C. Chen, W. L. Li, H. Q. Yao and J. Y. Xu, *Fitoterapia*, 2015, **103**, 231.
6 D. C. Blakemore, L. Castro, I. Churcher, D. C. Rees, A. W. Thomas, D. M. Wilson and A. Wood, *Nat. Chem.*, 2018, **10**, 383.
7 G. Li and H. X. Lou, *Med. Res. Rev.*, 2018, **38**, 1255.
8 Y. Q. Liu, J. Tian, K. Qian, X. B. Zhao, S. L. Morris-Natschke, L. Yang, X. Nan, X. Tian and K. H. Lee, *Med. Res. Rev.*, 2015, **35**, 1.
9 X. Zhang, K. P. Rakesh, C. S. Shantharam, H. M. Manukumar, A. M. Asiri, H. M. Marwani and H. L. Qin, *Bioorg. Med. Chem.*, 2018, **26**, 340.

10 Y. Mehellou, H. S. Rattan and J. Balzarini, *J. Med. Chem.*, 2017, **61**, 2211.
11 J. Rautio, H. Kumpulainen, T. Heimbach, R. Oliyai, D. Oh, T. Järvinen and J. Savolainen, *Nat. Rev. Drug Discovery*, 2008, **7**, 255.
12 S. Jana, S. Mandlekar and P. Marathe, *Curr. Med. Chem.*, 2010, **17**, 3874.
13 V. Abet, F. Filace, J. Recio, J. Alvarez-Builla and C. Burgos, *Eur. J. Med. Chem.*, 2017, **127**, 810.
14 Y. Q. Zheng, X. G. Ji, B. C. Yu, K. L. Ji, D. Gallo, E. Csizmadia, M. Y. Zhu, M. R. Choudhury, L. K. Cruz, V. Chittavong, Z. X. Pan, Z. N. Yuan, L. E. Otterbein and B. H. Wang, *Nat. Chem.*, 2018, **10**, 787.
15 S. S. Dhaneshwar and G. Vadnerkar, *Curr. Top. Med. Chem.*, 2011, **11**, 2318.
16 M. Roldo, E. Barbu, J. F. Brown, D. W. Laight, J. D. Smart and J. Tsibouklis, *Expert Opin. Drug Delivery*, 2007, **4**, 547.
17 S. H. Lee, E. Moroz, B. Castagner and J. C. Leroux, *J. Am. Chem. Soc.*, 2014, **136**, 12868.
18 J. Rao, C. Hottinger and A. Khan, *J. Am. Chem. Soc.*, 2014, **136**, 5872.
19 L. Zhang, Y. Wang, X. B. Zhang, X. Wei, X. Xiong and S. B. Zhou, *ACS Appl. Mater. Interfaces*, 2017, **9**, 3388.
20 X. M. Li, J. Y. Li, Y. Gao, Y. Kuang, J. Shi and B. Xu, *J. Am. Chem. Soc.*, 2010, **132**, 17707.
21 O. H. Nielsen and L. K. Munck, *Nat. Rev. Gastroenterol. Hepatol.*, 2007, **4**, 160.
22 R. B. Muijsers and K. L. Goa, *Drugs*, 2002, **62**, 1689.
23 I. B. Seiple, Z. Zhang, P. Jakubec, A. Langlois-Mercier, P. M. Wright, D. T. Hog, K. Yabu, S. R. Allu, T. Fukuzaki, P. N. Calsen, Y. Kitamura, X. Zhou, M. L. Condakes, F. T. Szczypiński, W. D. Green and A. G. Myers, *Nature*, 2016, **533**, 338.
24 C. F. Martinez-Farina, A. W. Robertson, H. Yin, S. Monro, S. A. McFarland, R. T. Syvitski and D. L. Jakeman, *J. Nat. Prod.*, 2015, **78**, 1208.
25 E. Fernández-álvaro, W. D. Hong, G. L. Nixon, P. M. O'Neill and F. Calderón, *J. Med. Chem.*, 2016, **59**, 5587.
26 M. Lamblin, R. Spingarn, T. T. Wang, M. C. Burger, B. Dabbas, N. Moitessier, J. H. White and J. L. Gleason, *J. Med. Chem.*, 2010, **53**, 7461.
27 A. Petrelli and S. Giordano, *Curr. Med. Chem.*, 2008, **15**, 422.
28 B. Al-Lazikani, U. Banerji and P. Workman, *Nat. Biotechnol.*, 2012, **30**, 679.
29 X. Dong and R. J. Mumper, *Nanomedicine*, 2010, **5**, 597.
30 N. Kolishetti, S. Dhar, P. M. Valencia, L. Q. Lin, R. Karnik, S. J. Lippard, R. Langer and O. C. Farokhzad, *Proc. Natl. Acad. Sci. U. S. A.*, 2010, **107**, 17939.
31 T. M. Sun, J. Z. Du, Y. D. Yao, C. Q. Mao, S. Dou, S. Y. Huang, P. Z. Zhang, K. W. Leong, E. W. Song and J. Wang, *ACS Nano*, 2011, **5**, 1483.
32 X. Guan, Y. Li, Z. Jiao, L. Lin, J. Chen, Z. Guo, H. Tian and X. Chen, *ACS Appl. Mater. Interfaces*, 2015, **7**, 3207.
33 T. Li, X. Shen, Y. Geng, Z. Chen, L. Li, S. Li, H. Yang, C. Wu, H. Zeng and Y. Liu, *ACS Appl. Mater. Interfaces*, 2016, **8**, 13748.
34 Y. Gao, L. Jia, Q. Wang, H. Hu, X. Zhao, D. Chen and M. Qiao, *ACS Appl. Mater. Interfaces*, 2019, **11**, 16296.
35 R. Wang, Z. Zhao, Y. Han, S. Hu, Y. Opoku-Damoah, J. Zhou, L. Yin and Y. Ding, *Mol. Pharmaceutics*, 2017, **14**, 2999.
36 H. Xu, M. Lv and X. Tian, *Curr. Med. Chem.*, 2009, **16**, 327.
37 Y. J. You, *Curr. Pharm. Des.*, 2005, **11**, 1695.
38 M. Gordaliza, P. A. Garcia, J. M. Miguel Del Corral, M. A. Castro and M. A. Gomez-Zurita, *Toxicon*, 2004, **44**, 441.
39 Z. Q. Wang, Y. H. Kuo, D. Schnur, J. P. Bowen, S. Y. Liu, F. S. Han, J. Y. Chang, Y. C. Cheng and K. H. Lee, *J. Med. Chem.*, 1990, **33**, 2660.
40 T. S. Huang, C. C. Lee, Y. Chao, C. H. Shu, L. T. Chen, L. L. Chen, M. H. Chen, C. C. Yuan and J. Whang-Peng, *Pharm. Res.*, 1999, **16**, 997.
41 J. M. Liu, L. T. Chen, Y. Chao, A. F. Y. Li, C. W. Wu, T. S. Liu, H. S. Shiah, J. Y. Chang, J. D. Chen, H. W. Wu, W. C. Lin, C. Lan and J. Whang-Peng, *Cancer Chemother. Pharmacol.*, 2002, **49**, 425.
42 W. Ha, X. B. Zhao, X. Y. Chen, K. Jiang and Y. P. Shi, *ACS Appl. Mater. Interfaces*, 2018, **10**, 21149.
43 K. H. Lee, S. A. Beers, M. Mori, Z. Q. Wang, Y. H. Kuo, L. Li, S. Y. Liu, J. Y. Chang, F. S. Han and Y. C. Cheng, *J. Med. Chem.*, 1990, **33**, 1364.
44 I. Mickuviene, V. Kirveliene and J. B. Uodka, *Toxicol. In Vitro*, 2004, **18**, 639.
45 T. C. Chou and P. Talalay, *Adv. Enzyme Regul.*, 1984, **22**, 27.
46 A. Khafif, S. P. Schantz, T. C. Chou, D. Edelstein and P. G. Sachs, *Carcinogenesis*, 1998, **19**, 419.
47 X. B. Zhao, W. Ha, K. Gao and Y. P. Shi, *Anal. Chem.*, 2020, **92**, 9039.
48 S. Saphier, A. Haft and S. Margel, *J. Med. Chem.*, 2012, **55**, 10781.
49 W. Kim, J. Nam, S. Lee, S. Jeong and Y. Jung, *Mol. Pharmaceutics*, 2016, **13**, 2126.
50 W. Ha, J. Yu, X. Y. Song, Z. J. Zhang, Y. Q. Liu and Y. P. Shi, *J. Mater. Chem. B*, 2013, **1**, 5532.
51 W. Ha, J. Yu, X. Y. Song, J. Chen and Y. P. Shi, *ACS Appl. Mater. Interfaces*, 2014, **6**, 10623.
52 M. Ceccato, P. L. Nostro and P. Baglioni, *Langmuir*, 1997, **13**, 2436.
53 I. N. Topchieva, A. E. Tonelli, I. G. Panova, E. V. Matuchina, F. A. Kalashnikov, V. I. Gerasimov, C. C. Rusa, M. Rusa and M. A. Hunt, *Langmuir*, 2004, **20**, 9036.
54 X. Song, Z. Zhang, J. Zhu, Y. Wen, F. Zhao, L. Lei, N. Phan-Thien, B. C. Khoo and J. Li, *Biomacromolecules*, 2020, **21**, 1516.
55 E. A. Günter and O. V. Popeyko, *Carbohydr. Polym.*, 2016, **147**, 490.
56 P. Wen, K. Feng, H. Yang, X. Huang, M. H. Zong, W. Y. Lou, N. Li and H. Wu, *Carbohydr. Polym.*, 2017, **169**, 157.
57 N. G. Kotla, M. Gulati, S. K. Singh and A. Shivapooja, *J. Controlled Release*, 2014, **178**, 55.
58 L. Zhao, X. Tian, P. C. Fan, Y. J. Zhan, D. W. Shen and Y. Jin, *J. Chromatogr. A*, 2008, **1210**, 168.
59 L. Zhao, Z. L. Liu, P. C. Fan, Z. W. Zhang, X. Liu, Y. J. Zhan and X. Tian, *J. Sep. Sci.*, 2009, 1323.